Petroleum and Coal

Article **Open Access**

An Accurate Model for Prediction of Wax Deposition in Oil Systems

Ali Barati-Harooni [1], Adel Najafi-Marghmaleki[1], Afshin Tatar [2], Armin Mohebbi [3], Abbas Khaksar-Manshad [4], Amir H Mohammadi [5,6]

[1] *Young Researchers and Elite Club, Ahvaz Branch, Islamic Azad University, Ahvaz, Iran*
[2] *Young Researchers and Elite Club, North Tehran Branch, Islamic Azad University, Tehran, Iran*
[3] *Young Researchers and Elite Club, South Tehran Branch, Islamic Azad University, Tehran, Iran*
[4] *Department of Petroleum Engineering, Abadan Faculty of Petroleum Engineering, Petroleum University of Technology (PUT), Abadan, Iran*
[5] *Discipline of Chemical Engineering, School of Engineering, University of KwaZulu-Natal, Howard College Campus, King George V Avenue, Durban, 4041, South Africa*
[6] *Institut de Recherche en Génie Chimique et Pétrolier (IRGCP), Paris Cedex, France*

Received June 18, 2017; Accepted September 30, 2017

Abstract

Wax deposition is a critical issue during the process of oil production in the petroleum industry. Hence, it is possible to enhance the quality and efficiency of oil production by using accurate and reliable models for estimation of wax deposition. This study highlights the application of radial basis function network optimized by genetic algorithm (GA-RBF) for pre-diction of wax deposition in oil systems based on literature data. The obtained results show that the proposed GA-RBF model is accurate and effective for prediction of target wax deposition data. In addition, the results of this work are compared with the results of CSA-LSSVM and multisolid thermodynamic models. The comparisons reveal that GA-RBF model presents more accurate results and outperforms other models for estimations of wax deposition.

Keywords: Wax; Genetic Algorithm (GA); Radial Basis Function (RBF); Multisolid thermos-dynamic model; Deposition.

1. Introduction

Wax deposition is one of the main unsolved challenges in flow assurance of pipelines and production equipment in the petroleum industry that can reduce oil production efficiency. It can result in blocking of wellbores, transportation pipelines, production equipment, and even reservoir rock and can significantly effect field economy, because of increasing operational and remedial costs in addition to the decrease of production rate [1-4]. In order to predict this solid deposition, an accurate, reliable, and well-detailed wax deposition and precipitation management program is needed, which can result in reducing of wax problems and remedial costs during oil production and transportation. In addition, prediction of deposited wax amount and temperatures of wax appearance (WAT) and wax disappearance (WDT), which has a great importance and value in designing of production processes can be achieved using a reliable and accurate model [2]. Therefore, the need for an appropriate model, which correctly predicts the amount of wax deposition, is clearly justified.

One of the frequently used thermodynamic models was developed by Burger *et al.* [5] in which dissolved the crude oil in a solvent mixture (ether/acetone) is cooled to 253K; in following it is filtrated at this temperature. The total amount of wax that can be deposited could be acceptably represented by this method [5]. Multisolid phase (MS) model is one of the most used thermodynamic methods in the literature [4,6]. Assuming each phase as a pure component, which does not mix with other phases of solid is one of the considerations of this model pre-sented by Lira-Galeana *et al.* [6]. Determination of wax deposition potential of three

waxy crude oils in a laminar flow of pipeline system was investigated by Valinejad and Solaimany Nazar [7]. They evaluated the impacts of important operation factors like inlet temperature of the crude oil, crude oil flow rate, and wax content, etc. by applying Taguchi experimental design approach [8]. Their obtained results indicate that more precipitated solid wax is caused with waxy crude oil containing higher wax content during transportation [7]. A novel method for modeling of wax deposition in fluid flow was developed by Akbarzadeh and Zougari [3]. Several possible mechanisms in the process of wax deposition were considered by them among which, particle diffusion/deposition was recognized as the main factor in deposits formation under actual transport conditions [4].

Determination yield stress of waxy oil gel created under quiescent and shear conditions was investigated by Bai and Zhang [9] using vane method [10]. Their results show that by increasing the average carbon number of wax, yield stresses dramatically decrease irrespective to quiescent or shear conditions [9]. An empirical model for prediction of wax precipitation in production systems was proposed by Kelechukwu *et al.* [11]. An acceptable prediction ability of this model compared with laboratory evaluation was exhibited.

Nevertheless, agreement of the predicted conditions of wax formation by thermodynamic models with experimental data is not excellent, and these predicted data and the wax precipitated amount are generally under- or overestimated [1]. On the other hand, in addition to special apparatus, expensive, challenging, and time-consuming procedures are required to perform experimental measurements. Accordingly, developing an accurate, reliable, and rapid method, which can resolve aforementioned thermodynamic models' problems and experimental measurements issues, is necessary. Some intelligent tools such as Fuzzy Logic (FL), Genetic Algorithm (GA), Artificial Neural Networks (ANNs), and Support Vector Machine (SVM) that are strongly reliable and powerful tools for data analysis and interpretation could be utilized to predict regression and assortment problems [12-25]. In this work, a radial basis function network optimized by genetic algorithm (GA-RBF) was developed for estimation of wax deposition in oil systems. In addition, the developed model was compared with other literature models. Results reveal that the developed model is accurate for estimation of wax deposi-tion and also is superior to other literature correlations.

2. Radial basis function neural network (RBF-NN)

ANNs gain their performance from the behavior of biological neurons [26]. The learning steps of these networks are done through iterative processes. The structure of these networks consists of parallel layers and interconnected units; hence, formulation of physical and mathematical relationships is not required [27-28]. The most important feature of neural networks is their ability for processing a large amount of data and their efficiency and capability to extend the results. ANNs are parallel distributed systems that consist of specific neurons as processing units. These units are located in layer(s) and transfer information between themselves by certain connections. Multi-layer Perceptron (MLP) and Radial Basis Function (RBF) networks are two well-known types of ANNs. Both models are the same in application because both of them are utilized for pattern recognition and nonlinear prediction. However, there are notable differences in their structure. RBF networks have several advantages over MLP networks such as the simple and fixed three layer structure, which brings them to be easier to design compared to MLP networks. They could react effectively to input noise; they also are capable to learn instantly and are able to effectively extend the results [29]. The high capability of RBF networks for generalization of results leads to their ability to figure out the patterns of testing data, which are not utilized in training process [30].

In modeling with RBF, the model tries to define a function f(x) to be able to accurately fit a *N*-dimensional data set, which contains a *D*-dimensional input vector such as $X^p=[X_i^p:1,2,...,N]$ to its corresponding output vector, t^p (i.e., $f(X^p)=t^p \ \forall p=1,...,D$). In RBFNs every data points have a basis function shown by $\phi(\|x-x^p\|)$ that $\phi(.)$ represents a

non-linear function. Next, by defining appropriate weight terms (w), the behavior and predictions of the network become close to the patterns, which exists in the data points. The weight terms appear in the fitting process by a mathematical formulation such as:

$$f(\mathrm{x}^q) = \sum_{p=1}^{N} w_p \phi(\left\| x^q - x^p \right\|) = \mathrm{t}^q \quad (1)$$

Taking into account this equation for all data points, it is possible to represent above equation in matrix form as $\phi W = t$ in which $t = \{\mathrm{t}^p\}$ and $W = \{\mathrm{w}^p\}$. Using matrix inversion techniques, the above equation is solvable by taking the form $W = \phi^{-1}\mathrm{t}$. Although there are various reports about the fact that certain features of function f(x) is independent to the RBFs ($\phi(r)$); however, one of the most useful and well-known types of RBFs is the Gaussian function formulated as follows:

$$\phi(\mathrm{r}) = \exp(-\frac{r^2}{2\sigma^2}) \quad (2)$$

where r>0 is the position of a data point x relative to a center c and the parameter σ evaluates the smooth behavior of function f(x). More details about RBF networks are available in the literature [21,31-32].

3. Genetic algorithm

The GA is a stochastic technique which originates based on Darwin's theory which states that in a population the better and fitter members and individuals have more chance to be survived [33-34]. This algorithm uses three basic operators in its optimization process. The name of these operators are selection, cross-over, and mutation [35]. The optimization process of GA to gain and characterize the best solution for a problem under consideration is controlled by using a cost function such as the Mean Square Error (MSE) between experimental data and model outcomes. The most important feature of GA is that it is free of derivative which means that stochastic and iterative searching nature of GA and its dynamic fitness evaluating performance introduces it as a powerful and robust optimization algorithm. This algorithm has a good capability for processing and dealing with non-continuous, non-differentiable, and nonlinear cost functions [34]. More details about this algorithm and its performance are available in the open literature [36-40].

4. Data acquisition

Table 1. Statistical parameters of the input and output parameters.

Parameter	Minimum	Maximum	Average
Wax deposition (wt%)	0	13	3.14
T (K)	230	314.15	272.66
Specific gravity	0.872	0.963	0.918
C_1-C_3 (%)	0.218	2.127	1.315
C_4–C_7 (%)	3.057	30.952	18.476
C_8–C_{15} (%)	33.468	49.791	44.495
C_{16}–C_{22} (%)	16.029	57.335	29.005
C_{23}–C_{29} (%)	0	10	2.811
C_{30+} (%)	0	13.23	3.538

In order to develop a reliable intelligent model, it is important to use reliable and valid data [41-49]. The data utilized should cover a wide range of variables. Hence, a data bank of 87 data points was collected from several published works and used in the present study [50-52]. The wax deposition was considered to be a function of nine parameters which reveal the thermodynamic features of corresponding oil systems. These parameters are the mole percentages of C_1-C_3, C_4–C_7, C_8–C_{15}, C_{16}–C_{22}, C_{23}–C_{29}, and C_{30+} components, temperature (T/K), and specific gravity. The details of the input and output parameters are listed in Table 1.

5. Results and discussion

5.1. Model development

The first normalization of data points between -1 and 1 was carried out using the following equation:

$$x_{Normal} = 2 \times \frac{x - x_{Min}}{x_{Max} - x_{Min}} - 1 \quad (3)$$

Then, to construct a reliable model for estimation of experimental solubility data, the gathered databank was randomly classified into two train and test data sets. The training data is essential for the construction of the initial structure of model, and the test data is utilized to evaluate the generalization ability and accuracy of the model in the estimation of unseen data (test data). To develop an RBF model, it is important to evaluate the tuned and optimized values of two para-meters corresponding to the structure of RBF model. The names of these parameters are Spread and Maximum Number of Neurons (MNN). It is of great importance to optimize these parameters because of their notable impact on the modeling ability of the model. Genetic Algo-rithm as a well-known optimization algorithm was used to optimize the values of Spread and MNN.

In the process of using GA for determining the optimum values of Spread and MNN, at first stage, a population size of 50 was constructed to tune the Spread and MNN values by GA. Next, the MSE value between target data and model outcomes was used as a cost function to sort the population and construction of new population. In the next step, the operators of GA including cross-over and mutation were applied to evaluate the optimum values of Spread and MNN. The MSE algorithm was controlled within the convergence of criterion of the model to optimum values as it is represented in Figure 1. The obtained values for Spread and MNN were 36 and 1.686, respectively.

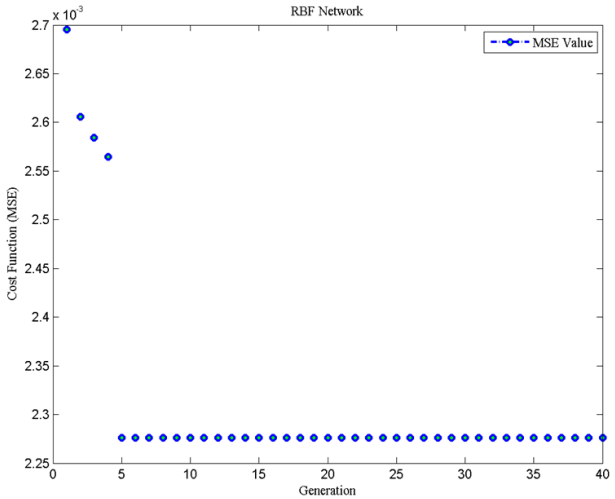

Figure 1. Convergence process of GA-RBF model to the optimum values of spread and MNN

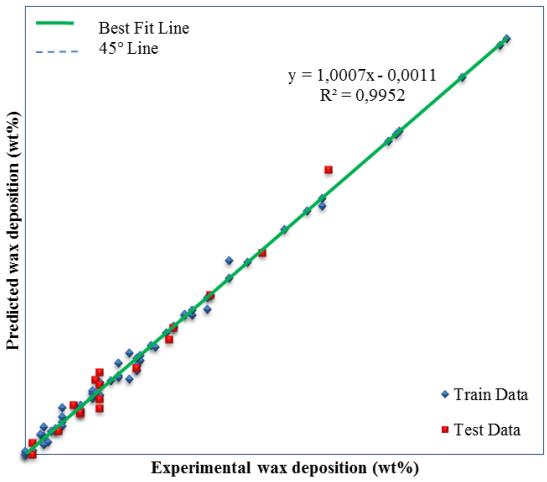

Figure 2. Estimated wax deposition values against experimental data

5.2. Evaluation of the model

Both graphical and statistical approaches were used to check the applicability and accuracy of the proposed model. For graphical validation, first, the regression plot is used. Figure 2 represents the regression plot of the GA-RBF method. The horizontal and vertical axes show the experimental and estimated values for wax deposition. The closer estimations to the target values lead to the aggregation of data points around the 45° line. As it is represented in Figure 2, both train and test data points are in a good degree of accuracy.

Another plot is the relative deviation plot of the model predictions. Figure 3 depicts the relative error deviation for the GA-RBF model. As it is clear, in the case of exclusion of 6 data points the maximum absolute relative deviation for GA-RBF is less than 0.4. To provide a proper view about the precision of the proposed model, the outcomes of the model and experimental values are simultaneously plotted in Figure 4. As it is clear, the esti-mated values are of excellent consistency with the experimental data.

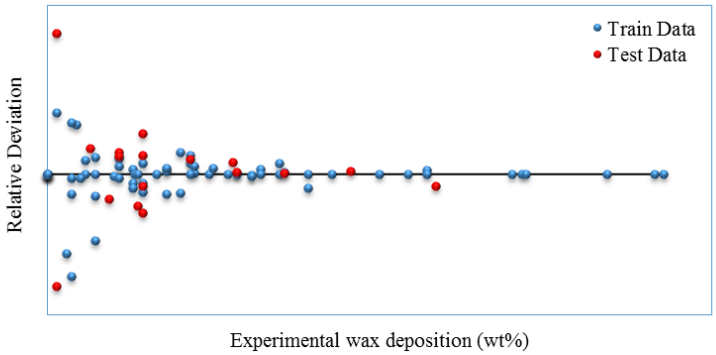

Figure 3. Relative deviations of the GA-RBF model against target wax deposition values

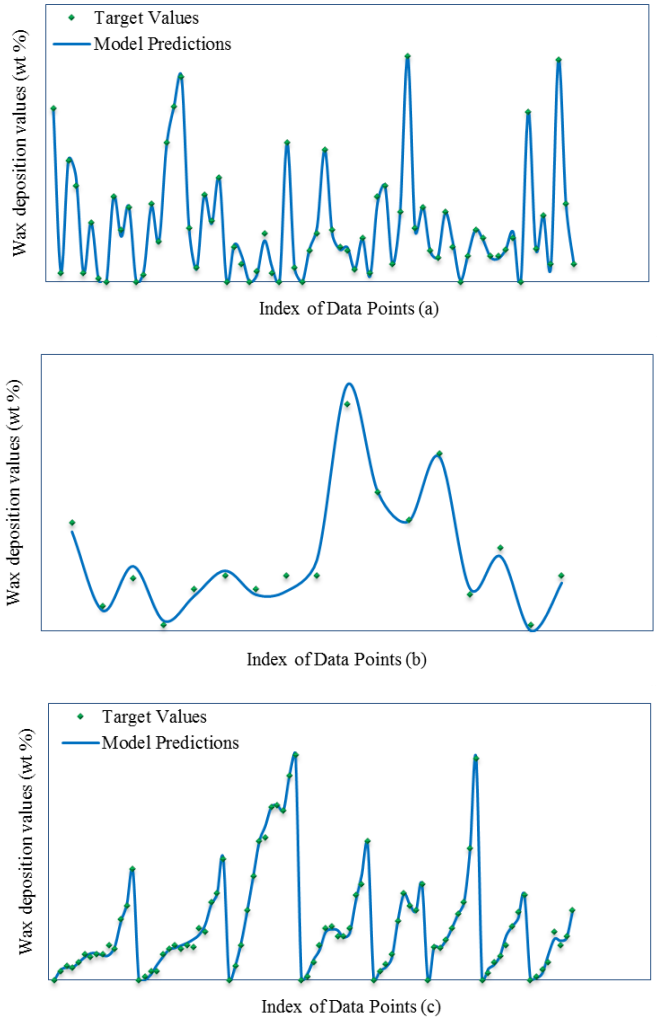

Figure 4. Co-representation of experimental and estimated wax deposition values versus index of data points

In case of statistical validation of the model, four statistical parameters of correlation factor (R^2), Average Absolute Relative Deviation (AARD), Standard Deviation (STD), and Root Mean Squared Error (RMSE) were used (Equations (4)-(7)). The mathematical representation of these parameters is as below:

$$R^2 = 1 - \frac{\sum_{i=1}^{N}(\lambda_{Pred}(i) - \lambda_{Exp}(i))^2}{\sum_{i=1}^{N}(\lambda_{Pred}(i) - \bar{\lambda}_{Exp})^2} \quad (4)$$

$$\%AARD = \frac{100}{N}\sum_{i=1}^{N}\left|\frac{(\lambda_{Pred}(i) - \lambda_{Exp}(i))}{\lambda_{Exp}(i)}\right| \quad (5)$$

$$RMSE = \left(\frac{\sum_{i=1}^{N}(\lambda_{Pred}(i) - \lambda_{Exp}(i))^2}{N}\right)^{0.5} \quad (6)$$

$$STD = \sum_{i=1}^{N}\left(\frac{(\lambda_{Pred}(i) - \bar{\lambda}_{Exp}(i))^2}{N}\right)^{0.5} \quad (7)$$

The calculated values for the train, test, and total phases are summarized in Table 2. The values of 0.99504, 11.33, 0.28, and 0.21 for respective R^2, AARD, STD, and RMSE for the total dataset show the reliability and ability of the developed GA-RBF model to reproduce the wax deposition values.

Table 2. The statistical parameters of the GA-RBF model for estimation of wax deposition

Data set	R^2	AARD%	STD	RMSE	N
Train data	0.9972	7.55	0.16	0.17	70
Test data	0.9791	26.90	0.51	0.34	17
Total data	0.9950	11.33	0.28	0.21	87

At this point of the study, the GA-RBF model is put into comparison with the previously published models. Kamari *et al.* [53] developed a CSA-LSSVM model for estimation of wax deposition using the same data bank as this study. Moreover, Lira-Galena *et al.* [6] developed a multisolid model for prediction of wax deposition using just data points related to oils 12 and 15 among all of the data points used in the present work. The multisolid model is explained in detail in Appendix A. First, the results of the GA-RBF model and the multisolid model proposed by Lira-Galena *et al.* [6] for oils 12 and 15 were compared as it is depicted in Figure 5 by plotting experimental and estimated wax deposition values against temperature for both models.

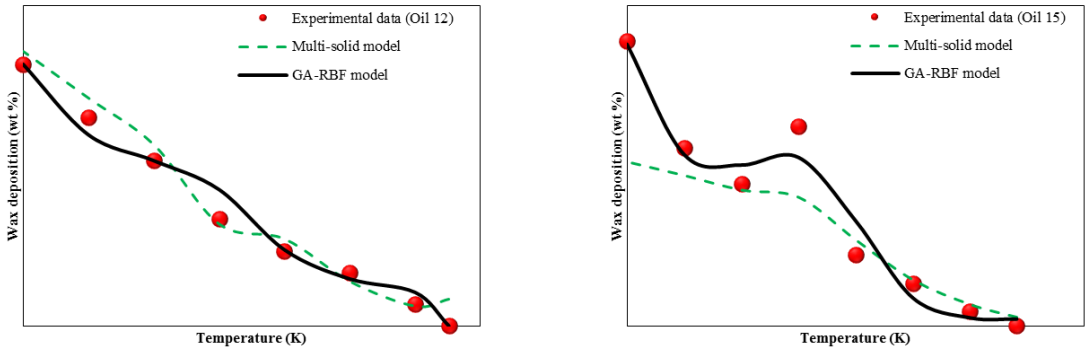

Figure 5. Comparison between the GA-RBF model and the multisolid model for estimation of wax deposi-tion values: (a) Oil 12, (b) Oil 15.

It is clear from this figure that the results of the GA-RBF model are accurate and more reliable than the multisolid model due to higher overlap between experimental values and the GA-RBF model results especially in the case of oil 15.

The comparison between the results of the GA-RBF model and the CSA-LSSVM model developed by Kamari *et al.* [53] is carried out by plotting the values of R^2, AARD, RMSE, and STD values of three methods at different phases of train, test, and total data points. These plots are depicted in Figure 6. It is clear from this figure that GA-RBF model outperforms this model thanks to higher values of R^2 and lower values of AARD, RMSE, and STD.

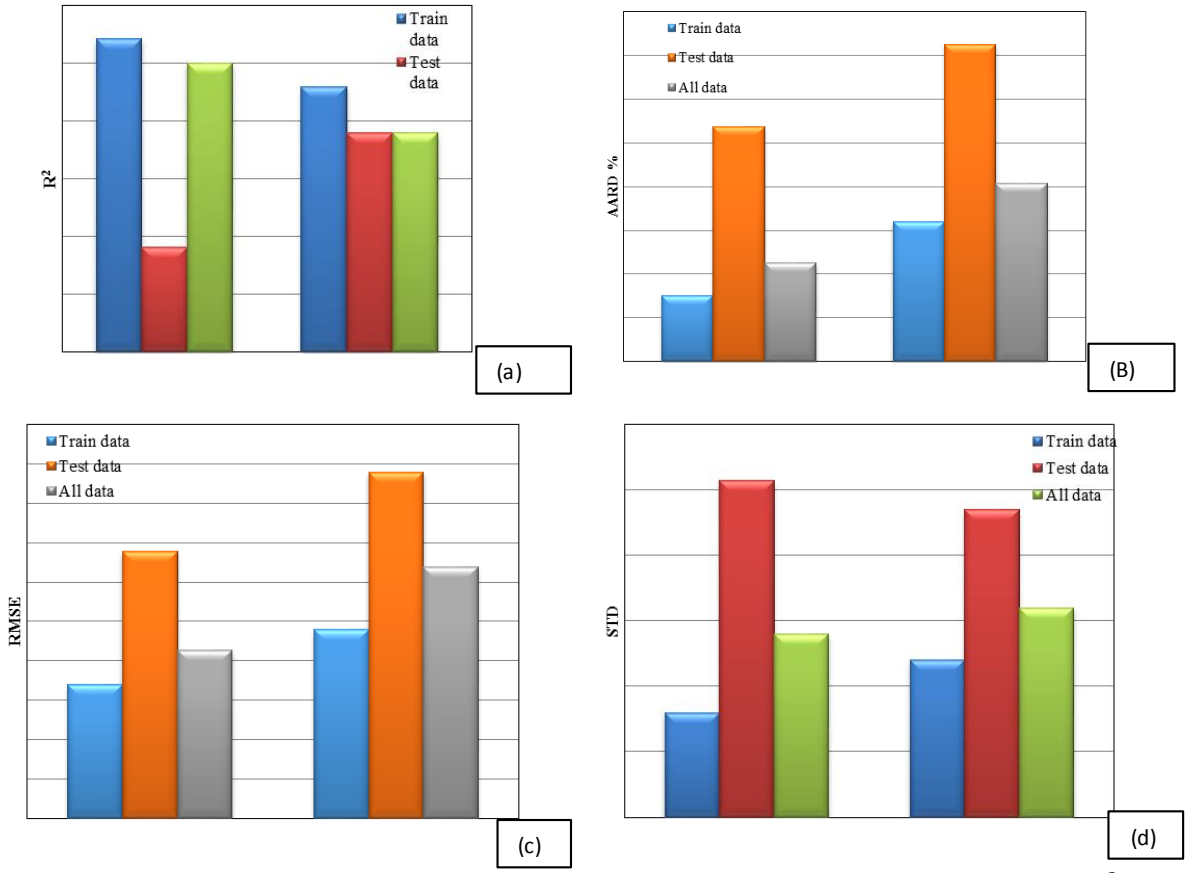

Figure 6. Comparison between results of the GA-RBF model and the CSA-LSSVM model: (a) R^2, (b) AARD, (c) RMSE, and (d) STD.

6. Conclusion

In this work, a GA-RBF model was developed for estimation of wax deposition in oil systems. The purpose of using genetic algorithm was to evaluate the optimum parameters related to the structure of RBF model and achieving the most accurate performance of the model. The outcomes of the model were put into comparison with experimental data by various statistical and graphical approaches to check the accuracy of the proposed GA-RBF model. Results reveal that the model is accurate and is capable to reproduce the target wax deposition values with the lowest possible error. The outcomes of the developed model were also compared with two literature models on wax deposition, and it is concluded that the GA-RBF model represents better results compared to other models. Results of this study could be used in areas where accurate predictions of wax deposition are necessary.

Appendix A. Multisolid thermodynamic model

This model assumes that when vapor-liquid-solid equilibrium exists in a system, the fugacities of a component such as component *i* in vapor, liquid, and solid phases are identical and the stability condition is valid. This leads to *N* vapor-liquid and N_s liquid-solid isofugasity equations as below:

$$f_i^v(P,T,y_1,y_2,...,y_{N-1}) - f_i^l(P,T,x_1,x_2,...,x_{N-1}) = 0;\ i = 1,2,...,N \qquad (A.1)$$

$$f_i^l(P,T,x_1,x_2,...,x_{N-1}) - f_{i,pure}^s(P,T) = 0;\ i = (N-N_s)+1,...,N \qquad (A.2)$$

In addition, for non-precipitating components there are a number of *N-1* material balance equations as below:

$$z_i - x_i^l\left[1 - \sum_j^{N_s}\frac{S_j}{F} - \frac{V}{F}\right] - K_i^{vl}x_i^l\frac{V}{F}f_i^l = 0;\ i = 1,...,(N-N_s) \qquad (A.3)$$

For precipitating components including pure solid phases, a number of N_s*-1* equations are valid as follows:

$$z_i - x_i^l\left[1 - \sum_j^{N_s}\frac{S_j}{F} - \frac{V}{F}\right] - K_i^{vl}x_i^l\frac{V}{F}f_i^l = 0;\ i = (N-N_s)+1,...,(N-1)\ (N_s > 1) \qquad (A.4)$$

where

$$K_i^{vl} = \frac{\phi_i^l(T,P,x^l)}{\phi_i^v(T,P,y)} \qquad (A.5)$$

$$f_i^l(T,P,z_j) - f_{pure,i}^s(T,P) \geq 0;\ i = 1,...,N \qquad (A.6)$$

In the above equations f_i^l represents the liquid fugacity of the *i-th* component, f_i^v is the vapor fugacity of the *i-th* component, *T* and *P* represent temperature and pressure, respectively, and the notations *x, y, z,* and *s* are related to respective mole percents of liquid, vapor, feed, and solid phases. It is possible to determine the onset of wax formations and the wax deposition value by simultaneously solving the above equations.

References

[1] Dalirsefat R, Feyzi F. A thermodynamic model for wax deposition phenomena. Fuel, 2007; 86: 1402-1408.

[2] Zuo JY, Zhang DD, Ng H-J. An improved thermodynamic model for wax precipitation from petroleum fluids, Chemical engineering science, 2001; 56: 6941-6947.

[3] Akbarzadeh K, Zougari M. Introduction to a novel approach for modeling wax deposition in fluid flows. 1. Taylor-Couette system, Industrial & Engineering Chemistry Research, 2008; 47: 953-963.

[4] Manshad AK, Ashoori S, Manshad MK, Omidvar P. The prediction of wax precipitation by the neural network and genetic algorithm and comparison with a multisolid model in crude oil systems, Petroleum Science and Technology, 2012; 30: 1369-1378.

[5] Burger E, Perkins T, Striegler J. Studies of wax deposition in the trans Alaska pipeline, Journal of Petroleum Technology, 1981; 33: 1,075-071,086.

[6] Lira-Galeana C, Firoozabadi A, Prausnitz JM. Thermodynamics of wax precipitation in petroleum mixtures, AIChE Journal, 1996; 42: 239-248.

[7] Valinejad R, Nazar ARS. An experimental design approach for investigating the effects of operating factors on the wax deposition in pipelines, Fuel, 2013; 106: 843-850.

[8] Mohammadi T, Moheb A, Sadrzadeh M, Razmi A. Separation of copper ions by electrodialysis using Taguchi experimental design, Desalination, 2004; 169: 21-31.

[9] Bai C, Zhang J. Effect of carbon number distribution of wax on the yield stress of waxy oil gels, Industrial & Engineering Chemistry Research, 2013; 52: 2732-2739.

[10] Liddel PV, Boger DV. Yield stress measurements with the vane, Journal of non-newtonian fluid mechanics, 1996; 63: 235-261.

[11] Kelechukwu EM, Al-Salim HS, Saadi A. Prediction of wax deposition problems of hydrocarbon production system, Journal of Petroleum Science and Engineering, 2013; 108: 128-136.
[12] Al-Anazi A, Gates I. A support vector machine algorithm to classify lithofacies and model permeability in heterogeneous reservoirs, Engineering Geology, 2010; 114: 267-277.
[13] Gharagheizi F, Alamdari RF, Angaji MT. A new neural network- group contribution method for estimation of flash point temperature of pure components, Energy & Fuels, 2008; 22: 1628-1635.
[14] Kaydani H, Mohebbi A, Baghaie A. Permeability prediction based on reservoir zonation by a hybrid neural genetic algorithm in one of the Iranian heterogeneous oil reservoirs, Journal of Petroleum Science and Engineering, 2011; 78: 497-504.
[15] Al-Anazi A, Gates I. Support vector regression to predict porosity and permeability: effect of sample size, Computers & Geosciences, 2012; 39: 64-76.
[16] Mohagheghi S, Arefi R, Ameri S, Rose D. Design and development of an artificial neural network for estimation of formation permeability, SPE Computer Applications, 1995; 7: 151-154.
[17] Lim J-S. Reservoir properties determination using fuzzy logic and neural networks from well data in offshore Korea, Journal of Petroleum Science and Engineering, 2005; 49: 182-192.
[18] Najafi-Marghmaleki A, Khosravi-Nikou MR, Barati-Harooni A. A new model for prediction of binary mixture of ionic liquids+ water density using artificial neural network, Journal of Molecular Liquids, 2016; 220: 232-237.
[19] Barati-Harooni A, Soleymanzadeh A, Tatar A, Najafi-Marghmaleki A, Samadi S-J. A Yari, B Roushani, Mohammadi AH. Experimental and modeling studies on the effects of temperature, pressure and brine salinity on interfacial tension in live oil-brine systems, Journal of Molecular Liquids, 2016; 219: 985-993.
[20] Barati-Harooni A, Najafi-Marghmaleki A, Tatar A, Mohammadi AH. Experimental and modeling study on adsorption of a nonionic surfactant on sandstone minerals in enhanced oil recovery process with surfactant flooding, Journal of Molecular Liquids, 2016; 220: 1022-1032.
[21] Tatar A, Nasery S, Bahadori M, Bahadori A, Bahadori M, Barati-Harooni A, Najafi-Marghmaleki A. Prediction of water removal rate in a natural gas dehydration system using radial basis function neural network, Petroleum Science and Technology, 2016; 34: 951-960.
[22] Manshad AK, Rostami H, Hosseini SM, Rezaei H. Application of Artificial Neural Network–Particle Swarm Optimization Algorithm for Prediction of Gas Condensate Dew Point Pressure and Comparison with Gaussian Processes Regression–Particle Swarm Optimization Algorithm, Journal of Energy Resources Technology, 2016;138: 032903.
[23] Toreifi H, Rostami H, Manshad AK. New method for prediction and solving the problem of drilling fluid loss using modular neural network and particle swarm optimization algorithm, Journal of Petroleum Exploration and Production Technology, 2014; 4: 371-379.
[24] Sayyad H, Manshad AK, Rostami H. Application of hybrid neural particle swarm optimization algorithm for prediction of MMP, Fuel, 2014; 116: 625-633.
[25] Manshad AK, Rostami H, Rezaei H, Hosseini SM. Application of artificial neural network-particle swarm optimization algorithm for prediction of asphaltene precipitation during gas injection process and comparison with Gaussian process algorithm, Journal of Energy Resources Technology, 2015; 137: 062904.
[26] Lin M-L, Chen C-W. RETRACTED: Stability analysis of community and ecosystem hierarchies using the Lyapunov method, Journal of Vibration and Control, 2011; 17: 1930-1937.
[27] Ahmadi MA, Ebadi M, Shokrollahi A, Majidi SMJ. Evolving artificial neural network and imperialist competitive algorithm for prediction oil flow rate of the reservoir, Applied Soft Computing, 2013; 13: 1085-1098.
[28] Bose NK, Liang P. Neural network fundamentals with graphs, algorithms, and applications, 2nd ed ed., McGraw-Hill, Inc., Boston, 1996.
[29] Santos RB, Rupp M, Bonzi SJ, Fileti AMF. Comparison Between Multilayer Feedforward Neural Networks and a Radial Basis Function Network to Detect and Locate Leaks in Pipelines Transporting Gas, Chem. Eng. Trans., 2013; 32: 1375-1380.

[30] Hao Y, Tiantian X, Paszczynski S, Wilamowski BM. Advantages of Radial Basis Function Networks for Dynamic System Design, Industrial Electronics, IEEE Transactions on, 2011; 58: 5438-5450.
[31] Naseri S, Tatar A, Shokrollahi A. Development of an accurate method to prognosticate choke flow coefficients for natural gas flow through nozzle and orifice type chokes, Flow Measurement and Instrumentation, 2016; 48: 1-7.
[32] Tatar A, Naseri S, Bahadori M, Hezave AZ, Kashiwao T, Bahadori A, Darvish H. Prediction of carbon dioxide solubility in ionic liquids using MLP and radial basis function (RBF) neural networks, Journal of the Taiwan Institute of Chemical Engineers, 2016; 60: 151-164.
[33] Holland JH. Adaptation in natural and artificial systems: an introductory analysis with applications to biology, control, and artificial intelligence, University of Michigan Press, USA, 1975.
[34] Magnier L, Haghighat F. Multiobjective optimization of building design using TRNSYS simulations, genetic algorithm, and Artificial Neural Network, Building and Environment, 2010; 45: 739-746.
[35] Shen C, Wang L, Li Q. Optimization of injection molding process parameters using combination of artificial neural network and genetic algorithm method, Journal of Materials Processing Technology, 2007; 183 412-418.
[36] Tatar A, Barati A, Yarahmadi A, Najafi A, Lee M, Bahadori A. Prediction of carbon dioxide solubility in aqueous mixture of methyldiethanolamine and N-methylpyrrolidone using intelligent models, International Journal of Greenhouse Gas Control, 2016; 47: 122-136.
[37] Tatar A, Yassin MR, Rezaee M, Aghajafari AH, Shokrollahi A. Applying a robust solution based on expert systems and GA evolutionary algorithm for prognosticating residual gas saturation in water drive gas reservoirs, Journal of Natural Gas Science and Engineering, 2014; 21: 79-94.
[38] Safari H, Nekoeian S, Shirdel MR, Ahmadi H, Bahadori A, Zendehboudi S. Assessing the Dynamic Viscosity of Na–K–Ca–Cl–H_2O Aqueous Solutions at High-Pressure and High-Temperature Conditions, Industrial & Engineering Chemistry Research, 2014; 53: 11488-11500.
[39] Ozcelik B, Erzurumlu T. Comparison of the warpage optimization in the plastic injection molding using ANOVA, neural network model and genetic algorithm, Journal of Materials Processing Technology, 2006; 171: 437-445.
[40] Azadeh A, Ghaderi S, Tarverdian S, Saberi M. Integration of artificial neural networks and genetic algorithm to predict electrical energy consumption, Applied Mathematics and Computation, 2007; 186: 1731-1741.
[41] Kamari A, Gharagheizi F, Shokrollahi A, Arabloo M, Mohammadi AH. Integrating a robust model for predicting surfactant–polymer flooding performance, Journal of Petroleum Science and Engineering, 2016; 137: 87-96.
[42] Kamari A, Arabloo M, Shokrollahi A, Gharagheizi F, Mohammadi AH. Rapid method to estimate the minimum miscibility pressure (MMP) in live reservoir oil systems during CO_2 flooding, Fuel, 2015; 153: 310-319.
[43] Shokrollahi A, Safari H, Esmaeili-Jaghdan Z, Ghazanfari MH, Mohammadi AH. Rigorous modeling of permeability impairment due to inorganic scale deposition in porous media, Journal of Petroleum Science and Engineering, 2015; 130: 26-36.
[44] Hemmati-Sarapardeh A, Alipour-Yeganeh-Marand R, Naseri A, Safiabadi A., Gharagheizi F, Ilani-Kashkouli P, Mohammadi AH. Asphaltene precipitation due to natural depletion of reservoir: Determination using a SARA fraction based intelligent model, Fluid Phase Equilibria, 2013; 354: 177-184.
[45] Esfahani S, Baselizadeh S, Hemmati-Sarapardeh A. On determination of natural gas density: least square support vector machine modeling approach, Journal of Natural Gas Science and Engineering, 2015; 22: 348-358.
[46] Shateri M, Ghorbani S, Hemmati-Sarapardeh A, Mohammadi AH. Application of Wilcoxon generalized radial basis function network for prediction of natural gas compressibility factor, Journal of the Taiwan Institute of Chemical Engineers, 2015; 50: 131-141.
[47] Rostami H, Manshad AK. Application of evolutionary Gaussian processes regression by particle swarm optimization for prediction of dew point pressure in gas condensate reservoirs, Neural Computing and Applications, 204; 24: 705-713.

[48] Manshad AK, Manshad MK, Ashoori S. Intelligent Modeling of Asphaltene Precipitation in Live and Tank Crude Oil Systems, Petroleum Science and Technology, 2012; 30: 1392-1403.
[49] Manshad AK, Keshavarz A. Prediction of the Amount of Asphaltene Precipitation by Fuzzy c-means Clustering, Energy Sources, Part A: Recovery, Utilization, and Environmental Effects, 2015; 37: 930-937.
[50] Pedersen WB, Hansen AB, Larsen E, Nielsen AB, Roenningsen HP. Wax precipitation from North Sea crude oils. 2. Solid-phase content as function of temperature determined by pulsed NMR, Energy & Fuels, 1991; 5: 908-913.
[51] Pedersen KSch, Skovborg P, Roenningsen HP. Wax precipitation from North Sea crude oils. 4. Thermodynamic modeling, Energy & Fuels, 1991; 5: 924-932.
[52] Hansen AB, Larsen E, Pedersen WB, Nielsen AB, Roenningsen HP. Wax precipitation from North Sea crude oils. 3. Precipitation and dissolution of wax studied by differential scanning calorimetry, Energy & Fuels, 1991; 5: 914-923.
[53] Kamari A, Khaksar-Manshad A, Gharagheizi F, Mohammadi AH, Ashoori S. Robust model for the determination of wax deposition in oil systems, Industrial & Engineering Chemistry Research, 2013; 52: 15664-15672.

To whom correspondence should be addressed: Dr. Abbas Khaksar-Manshad, Department of Petroleum Engi-neering, Abadan Faculty of Petroleum Engineering, Petroleum University of Technology, Abadan, Iran, E-mail: khaksar@put.ac.ir